Hydrogen-Bonding Clusters Leading to Formation of Supramolecular Dimers of Metalloporphyrin Receptors: Modulation of Lewis Acidity by π–π Interactions

Moshe Nakash,[a] Zöe Clyde-Watson,[a] Neil Feeder,[a] Simon J. Teat,[b] and Jeremy K. M. Sanders*[a]

Abstract: Two remarkable crystal structures are reported of a cyclic receptor **1**, containing two metalloporphyrin units. The overall crystal structure of **1** provides the first direct evidence that π-stacking between two metalloporphyrins reduces the Lewis acidity of the metal ion and thereby dramatically reduces the affinity of zinc for external ligands; this effect was previously suggested indirectly by solution state binding studies. In addition, crystallising **1** from a different combination of solvents and the ability of **1** to distort its structure leads to the remarkable observation of a supramolecular dimer of inter-penetrating macrocycles, **4**, held together by clusters of hydrogen-bonded methanol molecules.

Keywords: hydrogen bonds · metalloporphyrins · pi interactions · structure elucidation · supramolecular chemistry

Introduction

We report here on two remarkable crystal structures of the macrocyclic receptor **1** which was prepared as part of our larger study of porphyrin-accelerated Diels–Alder reactions.[1] We hope that by correlating the solid-state geometries revealed by X-ray crystal structures with solution-state kinetic and binding properties we will be able to construct a complete structure–activity relationship. However, unexpected bonuses from the structure determinations described here are the observations of a) reduction in the affinity of zinc porphyrins for external ligands due to π–π interaction, leading in this symmetrical macrocyclic receptor to methanol binding by only one of the two porphyrin moieties and b) a dimer of macrocycles held together by clusters of hydrogen-bonded methanol molecules.

Results and Discussion

Macrocycle **1** was synthesised as shown in Scheme 1.[2] Coupling the porphyrin monomer **2** to terephthaloyl chloride yielded the linear species **3**; deprotection and Glaser cyclisation gave **1** in overall yield of 16%. Small crystals of **1** were grown separately from a toluene/methanol mixture and from a dichloromethane/hexane/methanol mixture, and the structures were determined at station 9.8 on the synchrotron source at Daresbury (UK).

Macrocycle **1** (Figure 1) crystallises from a toluene/methanol mixture in the triclinic $P\bar{1}$ space group. The two porphyrin units in **1** are slightly domed[3] and are rotated by 30.0° with respect to each other (see Figure 1 top, left side). This rotation is likely to be facilitated, or required, by the relatively long diester chain linkage in **1**. The Zn–Zn distance in **1** is 12.045(2) Å. Only one of the two porphyrin units in **1** binds a methanol molecule. The intermolecular Zn–O bond length between the coordinating methanol molecule and the zinc atom in **1** is 2.18(4) Å (Figure 1). The zinc atom lies at a mean distance of 0.22(1) Å, above the N_4 plane (which is nearly coplanar, maximum deviation 0.002 Å) towards the oxygen atom. One more molecule of methanol is found in the cavity of **1** and is hydrogen-bonded to the zinc-coordinated methanol. The O···O distance of 2.68(1) Å, and the O···H distance between these two MeOH molecules are in the range typical for hydrogen bonding of the O–H···O type.[4, 5] For the non-coordinated porphyrin unit we detect, within experimental error, no displacement of the zinc atom from the N_4 plane. In addition, two molecules of toluene are trapped, one outside the cavity (filling some of the space between the various macrocycles in the crystal) and one inside the cavity (Figure 1).[6, 7]

Two enantiomeric receptors (due to twisting,[8] see above and Figures 1 and 2) are found in the unit cell of **1** and are

[a] Prof. J. K. M. Sanders, Dr. M. Nakash, Dr. Z. Clyde-Watson, Dr. N. Feeder
Cambridge Centre for Molecular Recognition
University Chemical Laboratory
Lensfield Road, Cambridge CB2 1EW (UK)
Fax: (+44) 1223-336017

[b] Dr. S. J. Teat
CLRC Daresbury Laboratory, Daresbury, Warrington, WA4 4AD (UK)
E-mail: jkms@cam.ac.uk

  0947-6539/00/0612-2112 $ 17.50+.50/0

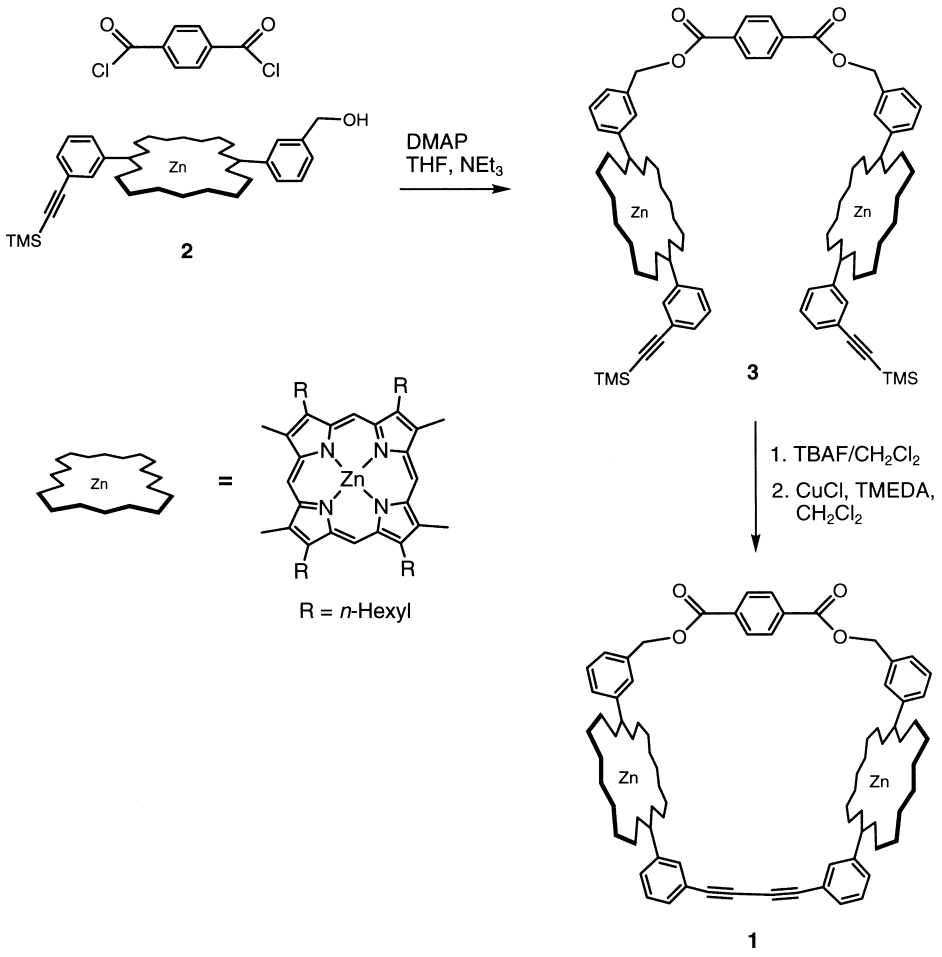

Scheme 1. Synthetic route to macrocycle **1**.

related to each other by inversion symmetry, forming an achiral crystal. One of the hexyl substituents on one of the porphyrin units (not shown) in **1** penetrates the cavity of an adjacent cyclic receptor (in the unit cell), while the other hexyl chains are accommodated in the gaps between the columns that run along the *a* axis in the unit cell (Figure 2). The porphyrin units in **1** do not penetrate the cavity of an adjacent receptor in the unit cell but their close proximity might account for the rotation, about the *meso* carbon axis, of the uncoordinated porphyrin unit in **1** (see Figures 1 and 2), creating a dihedral angle between the two N_4 planes of 17.9(1)°.

The overall crystal structure is composed of infinite columns which run along the *a* axis of the unit cell, in which each of the uncoordinated zinc porphyrin units forms an attractive π–π interaction with an adjacent receptor (see Figure 2 and Figure 3). Strong attractive interactions between the two porphyrin units lead to aggregation in solution.[9] Both in solution and crystals the two porphyrins generally adopt a cofacial arrangement with their centres offset.[10] This geometry may be summarised as follows: 1) The π systems of two neighbouring porphyrins are parallel, with an interplanar separation of 3.4–3.6 Å; 2) the π-stacked porphyrins are not rotated relative to one another, that is, their nitrogen–nitrogen axes are parallel; 3) one porphyrin is offset relative to the other by 3–4 Å along the nitrogen–nitrogen axis.[11] Figures 2 and 3 show the π-stacking relationships found in the crystal of **1**; the distance between the two N_4 planes of the two π–π interacting porphyrin units is 3.46(1) Å[12] and the relative orientation and offset are as expected for a strong attractive interaction.[10b, 11a] The fact that methanol is coordinated in **1** to only the zinc porphyrin unit which is *not* involved in π–π interaction, (see Figure 2), provides the first direct evidence that π stacking between two metalloporphyrins reduces the Lewis acidity of the metal ion and therefore dramatically reduces the affinity of zinc for external ligands, as was previously suggested from binding studies in solution.[10a] This reduction in Lewis acidity could be the result of a weak electrostatic interaction between the positive charge on the Zn atom,[13] in one porphyrin unit, and the π electrons in the other porphyrin unit.[11a, 14] This effect could account for the observation that one MeOH molecule found in the cavity of **1** prefers to form an intermolecular hydrogen bond with the Zn-coordinated MeOH molecule rather than to coordinate to the 'free' zinc atom in the porphyrin unit that is involved in the π–π interaction. In effect, this crystal structure appears to be the result of a competition between Zn–MeOH coordination and π–π interaction. For comparison, in the X-ray structure of complex **4** (see below and Figure 5), for which no π-π-interactions were found between porphyrin units of different complexes (see below and Figure 7), molecules of methanol are bound to both zinc atoms in both macrocycles **1a** and **1b** (Figure 4), that together form the complex **4**.[15]

Macrocycle **1** crystallises from dichloromethane/hexane/methanol mixture in the orthorhombic $P2_12_12_1$ space group, and in two closely related but not identical structural forms, **1a** and **1b** (see Figure 4), which together form the interpenetrated supramolecular dimer complex **4** (Figure 5). In both **1a** and **1b** one of the porphyrin units has a qualitatively planar structure, while the second porphyrin unit has a distorted saddle structure.[3] The two porphyrin moieties in **1a** and **1b** are rotated by 5.0° and 10.8° with respect to each other (see Figure 4 top, left side and right side, respectively) and are translated with respect to each other, due to a significant bending of the butadiyne linkage (see Figure 4 top and Figure 5 top). This molecular distortion results from a remarkable interpenetration of the pair of macrocycles to form complex **4**, which is stabilised by two hydrogen bonding

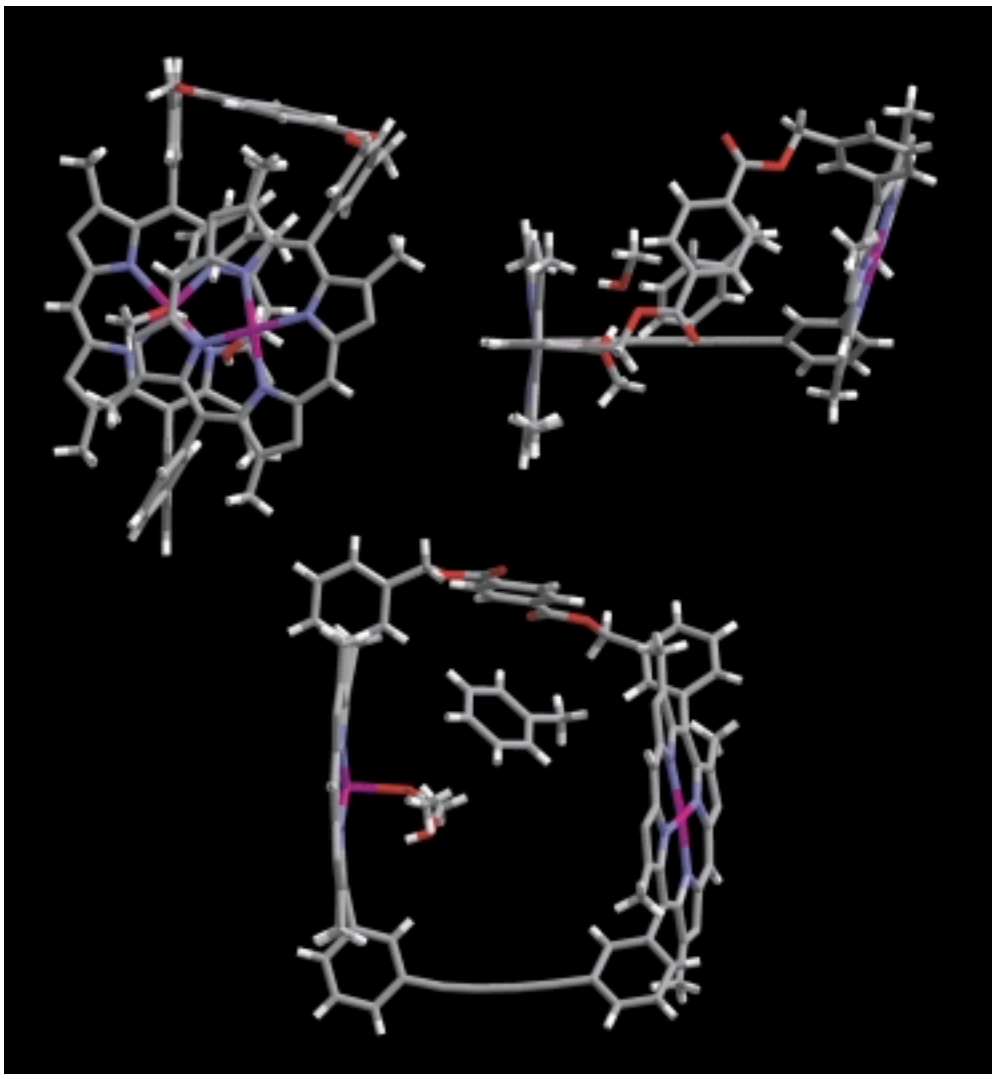

Figure 1. The molecular structure of **1**, side views (bottom and top left) and top view (top right). The coordinating MeOH molecule is shown together with the hydrogen bonded MeOH molecule and the trapped toluene molecule which are found in the cavity of **1**. The hexyl chains and the toluene molecule trapped outside the cavity have been omitted for clarity.

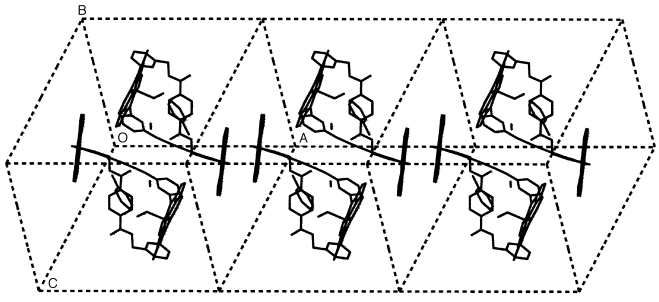

Figure 2. The relative arrangement of macrocycles **1** in the unit cell clearly showing the $\pi-\pi$ interactions between the porphyrins (drawn in a perpendicular orientation with respect to the paper plane) in the columns that run along the *a* axis. The alkyl substituents on the porphyrins, the hydrogen atoms and the toluene molecules trapped outside the cavity of macrocycle **1** have been omitted for clarity.

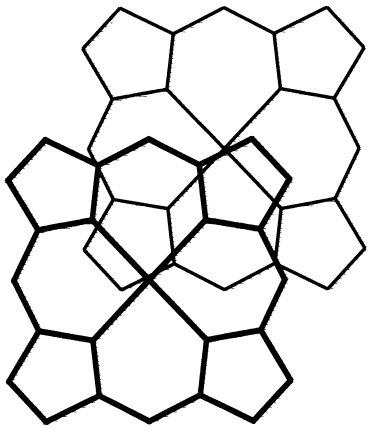

Figure 3. Side view of the $\pi-\pi$-interacting porphyrin pairs (in Figure 2), showing their relative orientation and offset. The alkyl substituents on the porphyrins and hydrogen atoms have been omitted for clarity.

arrays (see Figures 5 and 6) that connect the two macrocycles (**1a** and **1b**). This translation is likely to be facilitated by the relatively long diester linkage in **1**. The Zn–Zn distances in **1a** and **1b** are 11.808(3) Å and 11.898(3) Å, respectively, and are similar to that found in **1**, 12.045(2) Å (Figure 1).[16] The intermolecular Zn–O bond lengths between the coordinating methanol molecules and the zinc atoms Zn1, Zn2, Zn3 and

0947-6539/00/0612-2114 $ 17.50+.50/0 *Chem. Eur. J.* **2000**, *6*, No. 12

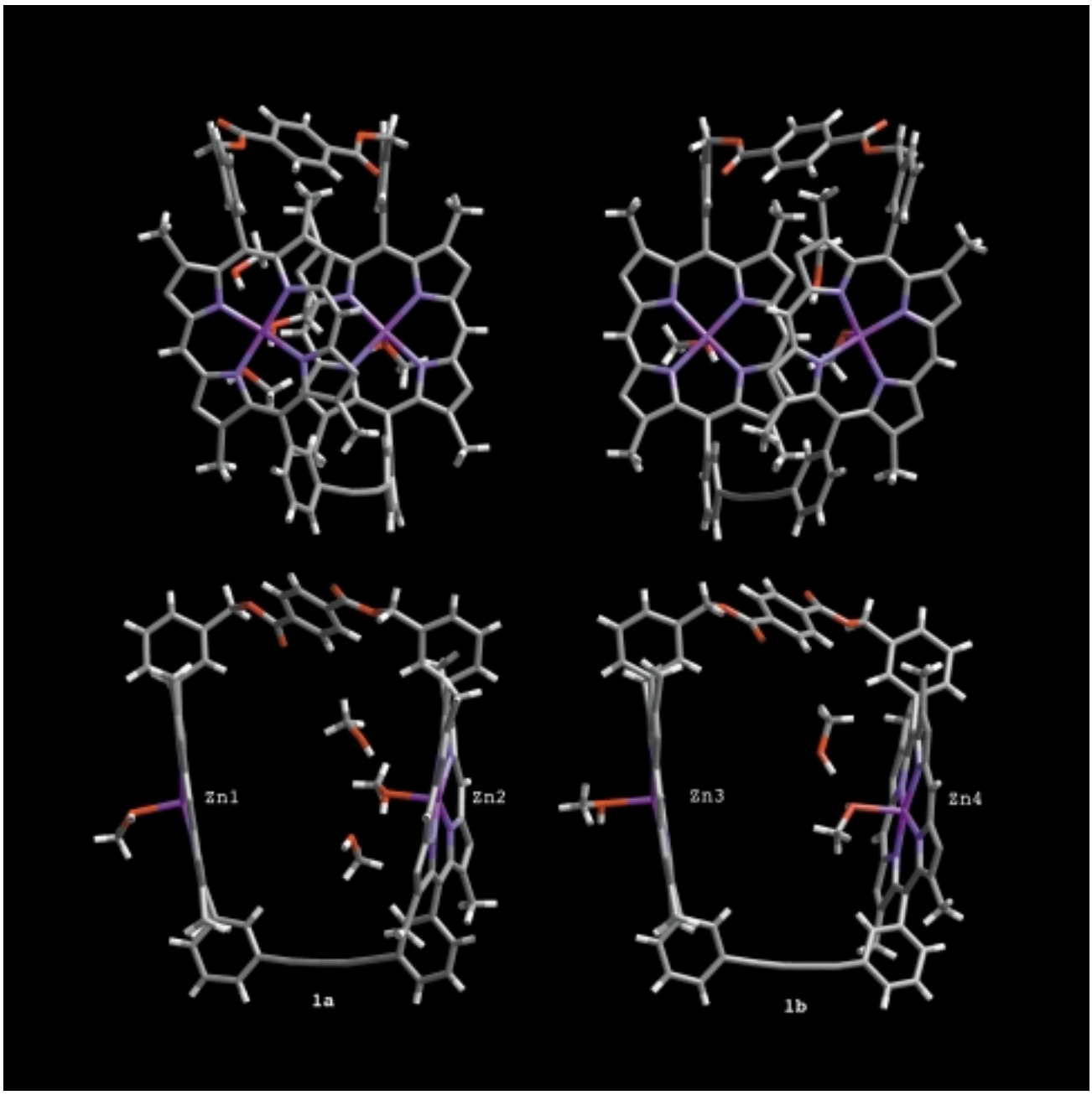

Figure 4. The molecular structure of the two structural forms of **1** (**1a** and **1b**; bottom: side view and top: top view) which together form the complex **4** (Figure 5). The coordinating MeOH molecules are also shown together with the hydrogen-bonded MeOH molecules which are found in the cavity of macrocycles **1a** and **1b**. The hexyl chains have been omitted for clarity. Macrocycle **1b** is drawn as shown in the complex **4** (Figure 5 bottom), while **1a** is rotated twice by 90° in two perpendicular motions, with respect to the way it is drawn in complex **4** (Figure 5 bottom).

Zn4 (Figure 4) are 2.20(2) Å, 2.20(2) Å, 2.20(2) Å and 2.22(2) Å, respectively. The zinc atoms Zn1, Zn2, Zn3 and Zn4 (Figure 4) lie at a mean distance of 0.23(1) Å, 0.21(1) Å, 0.22(1) Å and 0.22(1) Å, respectively, above the N_4 plane (which are nearly coplanar, maximum deviation 0.058 Å (left ring in **1a**), 0.018 Å (right ring in **1a**), 0.019 Å (left ring in **1b**) and 0.057 Å (right ring in **1b**)) towards the oxygen atom. The intermolecular Zn–O bonds lengths and the location of the Zn atom above the porphyrins N_4 planes in **4** are similar to those found in **1**. Macrocycles **1a** and **1b** differ in their structure also in the dihedral angles between the two N_4 planes (in each of these receptors), having angle values of 16.8(5)° and 20.9(5)°, respectively.

The formation of complex **4** in the solid state is facilitated by the flexibility of the framework, demonstrated by the marked deviation from twofold symmetry (in **1a** and **1b**) clearly seen in the relative orientations and translations of the porphyrin units in Figures 4 and 5. Complex **4** (Figure 5) consists of two interpenetrating cyclic metalloporphyrin receptors and seven hydrogen bonded methanol molecules, of which four are coordinated to the zinc porphyrins. Two of the hexyl substituents (not shown) on each of the two inner

  0947-6539/00/0612-2115 $ 17.50+.50/0

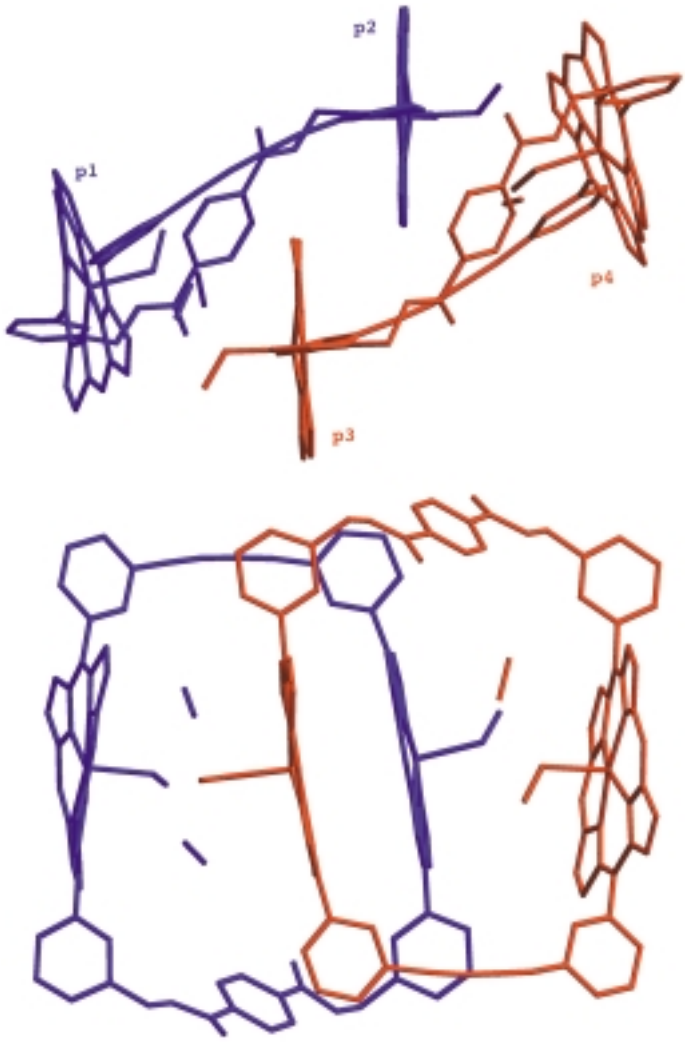

Figure 5. Side view (bottom) and top view (top) of the molecular structure of complex **4**. The alkyl substituents on the porphyrins and the hydrogen atoms have been omitted for clarity. p1, p2, p3 and p4 are symbols corresponding to the four porphyrin units in complex **4**.

'planar' porphyrin units, p2 and p3 (Figure 5), in complex **4** penetrate the cavity of the adjacent macrocycle (in the complex). Both **1a** and **1b** are chiral (due to bending and twisting,[8] see above and Figures 4 top and 5 top) and together form the supramolecular chiral complex **4**, which crystallises as a chiral crystal in the $P2_12_12_1$ space group.[17]

Hydrogen bonding clearly provides the driving force for the formation of complex **4**. Both **1a** and **1b** bind two methanol molecules intermolecularly (to the zinc porphyrin), one inside and one outside the cavity. These, in addition to the three other methanol molecules found in the complex, form two hydrogen-bonded arrays of four and three MeOH molecules in the space between porphyrins p1 and p3 and porphyrins p2 and p4, respectively (see Figure 5), and which hold the two macrocycles together. The O···H and O···O distances in the two hydrogen-bonded arrays in Figure 6 are in the range known for hydrogen bonding of the O–H···O type.[4, 18, 19] The two hydrogen-bonded arrays (Figure 6) are oriented in a homodromic manner, in which all the hydrogen bonds have the same circular direction. This orientation, which has also been found in other crystal structures,[20] is calculated to be lower in energy than the antidromic arrangement.[21] The higher relative rotation of the two porphyrins in **1b** (compared with **1a**) with respect to each other, see above, and the dihedral angle between the N_4 planes in porphyrins p2 and p3, 2.3(5)°, imposes a smaller free space between porphyrins p2 and p4 than in the case of porphyrins p1 and p3 (see Figure 5 top). This is reflected in a shorter Zn–Zn distance between porphyrins p2 and p4 versus porphyrins p1 and P3, 6.334(3) Å versus 6.973(3) Å, respectively. This might account for the observation that there are four methanol molecules in the space between porphyrins p1 and p3 while there are only three between porphyrins p2 and p4. The thermodynamic strength of a hydrogen bond is extremely variable, and for neutral molecules it normally lies in the range of 2–5 kcal mol^{-1}.[22] The two hydrogen-bonded arrays (Figures 5 and 6) are likely to be the dominant factor controlling the formation of complex **4**. We have previously detected clusters of hydrogen-bonded alcohols in the cavities of capped porphyrins in solution but not in crystals.[23] It is well known that the stronger hydrogen-bond motifs found in organic systems can be used to direct the synthesis of supramolecular complexes, for example in crystal engineering.[22, 24] It is also known that hydrogen bonds between solvent and solute molecules facilitate the retention of organic solvents in crystals.[25]

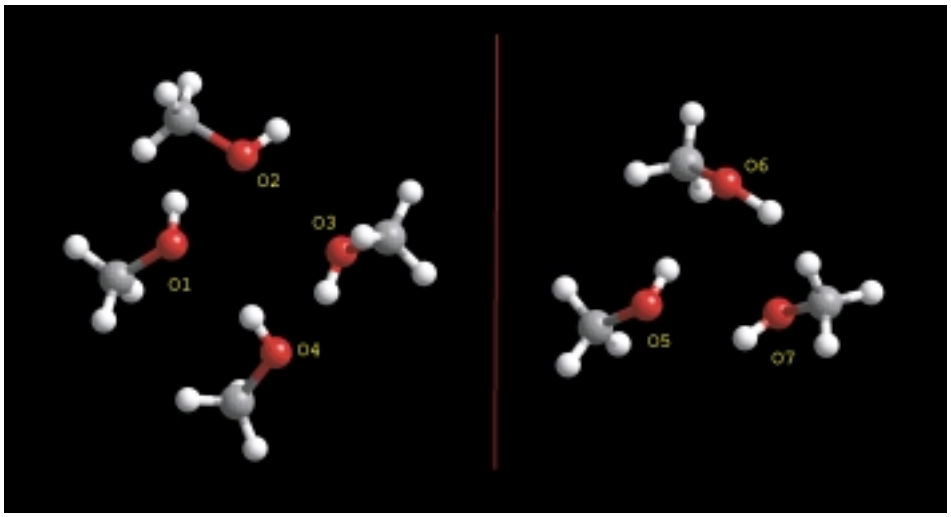

Figure 6. The two homodromic hydrogen-bonded arrays found in **4**. The four MeOH array (left) and the three MeOH array (right) lie in the space between porphyrins p1 and p3 and porphyrins p2 and p4, respectively (see Figure 5 top). The oxygen–oxygen distances are: O1–O2 2.58(2), O2–O3 2.66(2), O3–O4 2.70(2), O4–O1 2.89(3), O5–O6 3.20(3), O6–O7 2.77(3), and O7–O5 2.82(3) Å. The oxygen atoms that are bound to the Zn-porphyrin units in complex **4** are: O1, O3, O5, and O7.

The two planar porphyrins p2 and p3 in complex **4** (see Figure 5) are almost parallel, with interplanar separation of 3.5 Å[26] and are just slightly rotated (1.2°) relative to one

0947-6539/00/0612-2116 $ 17.50+.50/0 *Chem. Eur. J.* **2000**, *6*, No. 12

another, as expected for π–π interaction between porphyrins (see above).[10, 11a, 27] However, porphyrins p2 and p3 are 7.5 Å offset relative to one another, mainly along the meso carbons axis. This offset is expected to significantly reduce the favourable π–π interaction between the two porphyrin units,[11a] p2 and p3. Therefore, the possible weak π–π interaction between porphyrins p2 and p3 (if it exists at all, given the geometrical relationship) is not expected to stabilise the complex significantly. The formation of complex **4** is likely to be driven by the seven hydrogen bonds (see Figures 5 and 6) which give a maximum of less than about 20–35 kcal mol^{-1} of stability to the complex. However, as complex **4** consists of some nine molecules the entropic penalty for its assembly in solution will be very large: the equilibrium constant for dimerization will therefore be too small to observe experimentally in solution at accessible concentrations but is clearly enough to control the mode of crystallisation.

The overall crystal structure of complex **4** is composed of layers of inter-penetrating dimers of cyclic zinc-porphyrin receptors parallel to the plane defined by the *a* and *c* axes of the unit cell. These layers reveal that each complex is surrounded by another six dimeric complexes and that there are no π–π interactions between porphyrin units of different complexes, so each complex is an 'autonomic' unit (Figure 7). As the crystal of complex **4** is chiral, a side view of these layers show 'spiral columns' that have the same directionality. Large channels run between the layers throughout the crystal parallel to the *a* axis, which accommodate most of the hexyl substituents on the porphyrin units.

By comparison with conventional small molecule crystallography, the *R* factors associated with structures **1** and **4** are rather large. This is hardly surprising: the large unit cell and lack of heavy atoms ensure that the X-ray scattering power of the crystals will be very low,[28] while the four solubilising hexyl chains per porphyrin unit tend to be disordered; furthermore, solvent molecules are often included within and between molecules in the lattice. In general therefore, we have needed recourse to synchrotron sources of X-rays. It is important to note that although the large *R* factors associated with this kind of system inevitably limit the precision with which one can determine bond lengths and angles, they do not detract from our ability to draw conclusions about intermolecular interactions or large scale molecular distortions.

Conclusion

The results presented here show that macrocycle **1** is rather flexible and able to respond to weak interactions and ligands by distorting the porphyrin framework and by torsion around the butadiyne linkage. The efficiency of **1** in accelerating the recently studied Diels–Alder reaction[1b] will be tested as part of a structure–activity relationships study for a series of different but closely related macrocycles that are now being prepared in our laboratory. The overall crystal structure of **1** gives the first direct evidence that π stacking between two metalloporphyrins reduces the Lewis acidity of the metal ion and therefore dramatically reducing the affinity of zinc for external ligands, as was previously suggested from binding studies.[10a] In addition, crystallising **1** from a different combination of solvents and the ability of **1** to distort its structure (as seen in **1a** and **1b**) leads to the remarkable

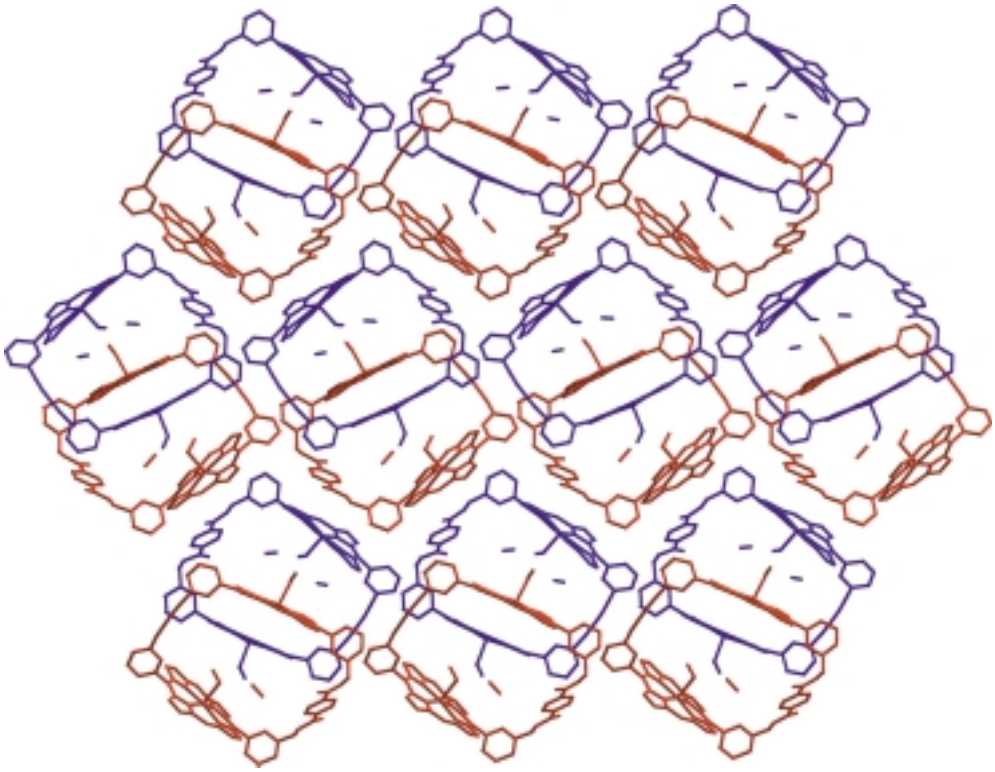

Figure 7. The relative arrangement of the dimeric complexes **4** in the crystal layers, parallel to the plane defined by the *a* and *c* axes of the unit cell. The alkyl substituents on the porphyrins and the hydrogen atoms have been omitted for clarity.

observation of a supramolecular dimer of inter-penetrating metalloporphyrin macrocycles, **4**, held together by clusters of hydrogen-bonded methanol molecules.

Experimental Section

General: ^{1}H NMR spectra (250 MHz) were recorded on Bruker AC-250 spectrometers. ^{13}C NMR spectra were obtained on a Bruker AC-250 operating at 62.5 MHz. All NMR measurements were carried out at room temperature in deuterochloroform. MALDI-TOF mass spectra were recorded on a Kratos Analytical Ltd, Kompact MALDI IV mass spectrometer. A nitrogen laser (337 nm, 85 kW peak laser power, 3 ns pulse width) was used to desorb the sample ions, and the instrument was operated in linear time of flight mode with an accelerating potential of 20 kV. Results from 50 laser shots were signal averaged to give one spectrum. An aliquot (1 μL) of a saturated solution of the matrix (sinapinic acid) was deposited on the sample plate surface. Before the matrix completely dried, a small volume (1 μL) of analytes (dissolved in dichloromethane/chloroform at 1 mg mL^{-1}) was layered on the top of the matrix and allowed to air-dry.

Spectroscopic data for 1: Receptor **1** was prepared from monomer **2** according to the general procedure[2] with an overall yield of 16 %. ^{1}H NMR (250 MHz, $CDCl_3$): $\delta = 0.75 - 0.82$ (m, 24 H; hexyl Me), 1.13 – 1.42 (m, 32 H; hexyl CH_2), 1.51 – 1.66 (m, 16 H; hexyl CH_2), 1.97 (m, 16 H; hexyl CH_2), 2.27 – 2.34 (m, 24 H; ring Me), 3.75 (m, 16 H; CH_2-Por), 5.51 (s, 4 H; benzyl CH_2), 7.55 (s, 2 H; aryl-H), 7.63 – 7.88 (m, 12 H; aryl-H), 8.19 (m, 2 H; aryl-H), 8.37 (d, ^3J(H, H) = 7.3 Hz, 2 H; aryl-H) 9.88 (s, 4 H; *meso*-H); ^{13}C NMR (62.5 MHz, $CDCl_3$, APT): $\delta = 13.95$, 15.17, 15.56 (Me), 22.59, 26.57, 29.86, 31.79, 33.15 (hexyl CH_2), 67.67 (benzyl CH_2), 74.46, 83.26 (C≡C), 97.16 (*meso*), 116.90, 118.07, 120.88, 133.69, 134.54, 137.11, 137.33, 143.23, 143.35, 144.42, 144.72, 146.10, 146.12, 147.12, 147.32 (quaternary pyrrole and aryl carbons), 127.05, 127.32, 128.45, 129.42(× 3), 133.26, 133.47, 139.74 (aryl-H), 165.75 (ester C=O); MALDI-TOF MS ($C_{134}H_{160}N_8O_4Zn_2$) calculated: 2073.114, found: 2073.1.

X-ray crystallography: After much effort, only small crystals of **1** and **4** could be grown. These proved to be weakly diffracting with a laboratory X-ray source. In order to determine the structure it was necessary to exploit the high intensity of a synchrotron radiation source. Data were collected at the Daresbury SRS (UK), Station 9.8[29, 30] using a Bruker AXS Smart CCD area-detector diffractometer, in narrow frame mode. Intensities were integrated[31] from several series of exposures. For **1** each exposure covered 0.3° in ω, with an exposure time of 1 s and the total data set was more than a hemisphere. For **4** each exposure covered 0.2° in ω, with an exposure time of 10 s and the total data set was more than a quadrant. Data were corrected for absorption and incident beam decay.[32] The unit cell parameters were refined using LSCELL.[33]

Even using a synchrotron radiation source, these crystals were found to be weakly diffracting because of extensive disorder of the *n*-hexyl chains. This resulted in relatively high R1 values. Experience with this type of structure[34, 35] has shown that the particular refinement stratagem employed to model the chains depends on the degree of disorder and the quality of the diffraction data.

In both structures it was possible to locate two separate conformations for many of the *n*-hexyl chains. The relative occupancy of the two conformations was determined by first fixing the temperature factors of the atoms concerned to some reasonable value. Their site occupancy values were then refined, with common values for the atoms within one conformation, but constrained such that the sum between the two conformations was equal to 1. The occupancy of the chains was then fixed at those values and the carbon atoms allowed to refine with isotropic temperature factors. For the structure **4** the data was particularly weak and the disorder severe. In this case, carbon atoms at the same position in each chain were refined with common isotropic temperature factors. The data collected from the crystal of **1** was of slightly better quality and it was possible to allow the isotropic temperature factors of the atoms in the chains to refine independently. For all the *n*-hexyl chains, it was necessary to impose some restraints on the 1,2 and 1,3 C–C bond lengths in order to produce groups with a sensible geometry. The two toluene molecules located in the structure **1** were both disordered. One molecule was disordered about an inversion center. The second was modelled over two overlapping sites, with occupancies of 0.6 and 0.4 respectively. Crystallographic data (excluding structure factors) for the structures reported in this paper have been deposited with the Cambridge Crystallographic Data Centre as supplementary publication no. CCDC-119695 (for **1**) and CCDC-116960 (for **4**). Copies of the data can be obtained free of charge on application to CCDC, 12 Union Road, Cambridge CB2 1EZ, UK (fax: (+44) 1223 336-033; e-mail: deposit@ccdc.cam.ac.uk).

Crystal data for 1: $C_{146.50}H_{176}N_8O_6Zn_2$, $M_r = 2275.69$, crystal dimensions 0.24 × 0.18 × 0.10 mm, triclinic, space group $P\bar{1}$ (no. 2) $a = 18.8040(10)$, $b = 18.8570(10)$, $c = 20.6530(10)$ Å $\alpha = 92.560(10)$, $\beta = 115.680(10)$, $\gamma = 104.280(10)°$, $V = 6299.0(6)$ Å^3, $Z = 2$, $\rho_{calcd} = 1.200$ Mg m^{-3}, $\mu = 0.440$ mm^{-1}, $\theta_{max} = 29.49°$, $Mo_{K\alpha}$, $\lambda = 0.6884$ Å, $T = 150(2)$ K. A total of 60337 measured reflections of which 32382 were independent [R(int) = 0.0615]. Final residuals (32382 included reflections, 1381 parameters) $R1[I > 2\sigma(I)] = 0.0922$, $wR2 = 0.2197$, $S = 1.090$, ($w = 1/[\sigma^2F_o^2 + (0.0835P)^2 + 12.875P]$ where $P = (F_o^2 + 2F_c^2)/3$)). Largest peak and hole in the difference map − 1.067 and − 0.649 e Å^{-3}, respectively. The structure was solved by direct methods using SIR-92[36] and refined with SHELXL-97.[37]

Crystal data for complex 4: $C_{137.50}H_{170}N_8O_{7.50}Zn_2$, $M_r = 2185.55$, crystal dimensions 0.10 × 0.06 × 0.04 mm. Orthorhombic, space group $P2_12_12_1$(no. 19) $a = 19.2330(10)$, $b = 33.403(2)$, $c = 37.607(2)$ Å, $V = 24160(2)$ Å^3, $Z = 8$, $\rho_{calcd} = 1.202$ Mg m^{-3}, $\mu = 0.457$ mm^{-1}, 2θmax = 45.2°, synchrotron radiation $\lambda = 0.6887$ Å, $T = 150(2)$ K. A total of 52108 measured reflections of which 34001 were independent [$R_{(int)} = 0.0742$]. Final residuals (34001 included reflections; 1229 parameters) $R1[I > 2\sigma(I)] = 0.1673$, $wR2 = 0.3872$, $S = 1.160$, ($w = 1/[\sigma^2F_o^2 + (0.161P)^2 + 223.264P]$ where $P = (F_o^2 + 2F_c^2)/3$)). Largest peak and hole in the difference map 1.654 and − 1.164 e Å^{-3}, respectively. The structure was solved by direct methods using SIR-92[36] and refined with SHELXL-97.[37]

Acknowledgements

We thank the EPSRC, British Council, Israel Academy and Ministry of Science, and B'nai B'rith for financial support.

[1] a) Z. Clyde-Watson, A. Vidal-Ferran, L. J. Twyman, C. J. Walter, D. W. J. McCallien, S. Fanni, N. Bampos, R. S. Wylie, J. K. M. Sanders, *New J. Chem.* **1998**, *22*, 493 – 502; b) M. Marty, Z. Clyde-Watson, L. J. Twyman, M. Nakash, J. K. M. Sanders, *Chem. Commun.* **1998**, 2265 – 2266; c) M. Nakash, Z. Clyde-Watson, N. Feeder, J. E. Davies, S. J. Teat, J. K. M. Sanders, *J. Am. Chem. Soc.* **2000**, *122*, in press.

[2] The general route is described in: L. J. Twyman, J. K. M. Sanders, *Tetrahedron Lett.* **1999**, *40*, 6681 – 6684.

[3] For definitions and energies of different types of porphyrin distortions see: a) D. J. Nurco, C. J. Medforth, T. P. Forsyth, M. M. Olmstead, K. M. Smith, *J. Am. Chem. Soc.* **1996**, *118*, 10918 – 10919; b) W. Jentzen, M. C. Simpson, J. D. Hobbs, X. Song, T. Ema, N. Y. Nelson, C. J. Medforth, K. M. Smith, M. Veyrat, M. Mazzanti, R. Ramasseul, J.-C. Marchon, T. Takeuchi, W. A. Goddard, III, J. A. Shelnutt, *J. Am. Chem. Soc.* **1995**, *117*, 11085 – 11097.

[4] For the geometry of hydrogen bonding see: a) F. H. Allen, W. D. S. Motherwell, P. R. Raithby, G. P. Shields, R. Taylor, *New J. Chem.* **1999**, *23*, 25 – 34; b) G. A. Jeffrey, W. Saenger, '*Hydrogen Bonding in Biological Structures*', Springer, Berlin, **1991**.

[5] As the precision in the location of hydrogen atoms is less than for oxygen atoms, we present the O ··· O distances.

[6] An X-ray structure for a toluene-solvated porphyrin has been reported; W. R. Scheidt, M E. Kastner, K. Hatano, *Inorg. Chem.* **1978**, *17*, 706 – 710.

[7] In some host systems, inclusion of solvent molecules and their displacement by a single ligand guest molecule was suggested as the main driving force for binding and acceleration of bimolecular reactions: a) J. Kang, J., Jr. Rebek, *Nature* **1996**, *382*, 239 – 241; b) J. Kang, J. Santamaria, G. Hilmersson, J. Jr. Rebek, *J. Am. Chem. Soc.* **1998**, *120*, 7389 – 7390.

  0947-6539/00/0612-2118 $ 17.50+.50/0

[8] For other examples of chiral structures in crystals formed due to a twist see: a) D. G. Hamilton, J. E. Davies, L. Prodi, J. K. M. Sanders, *Chem. Eur. J.* **1998**, *4*, 608–620; b) R. G. Chapman, G. Olovsson, J. Trotter, J. C. Sherman, *J. Am. Chem. Soc.* **1998**, *120*, 6252–6260; c) J. R. Fraser, B. Borecka, J. Trotter, J. C. Sherman, *J. Org. Chem.* **1995**, 60, 1207–1213; d) D. J. Cram, M. E. Tanner, C. B. Knobler, *J. Am. Chem. Soc.* **1991**, *113*, 7717–7727; e) D. O'Krongly, S. R. Denmeade, M. Y. Chiang, R. Breslow, *J. Am. Chem. Soc.* **1985**, *107*, 5544–5545.

[9] a) A. E. Alexander, *J. Chem. Soc.* **1937**, 1813–1816; b) A. Hughes, *Proc. R. Soc. London, Ser. A* **1936**, *155*, 710–711; c) R. J. Abraham, F. Eivazi, H. Pearson, K. M. Smith, *J. Chem. Soc. Chem. Commun*. **1976**, 698–699; d) R. J. Abraham, F. Eivazi, H. Pearson, K. M. Smith, *J. Chem. Soc. Chem. Commun*. **1976**, 699–701.

[10] a) C. A. Hunter, P. Leighton, J. K. M. Sanders, *J. Chem. Soc. Trans. Perkin 1* **1989**, 547–552; b) W. R. Scheidt, Y. Lee, *Structure Bonding, Vol. 64,* Springer, Heidelberg, **1987**.

[11] a) C. A. Hunter, J. K. M. Sanders, *J. Am. Chem. Soc.* **1990**, *112*, 5525–5534; b) This offset of 3–4 Å along the nitrogen-nitrogen axis is the optimal calculated energy structure for π-stacking in porphyrins and is an arrangement found in many crystal structures of porphyrins.[10, 11a] However, deviations (in value and the direction) from this offset are also known in the solid state.[10b]

[12] Calculated as the distance between the N_4-plane in one porphyrin unit and one of the nitrogen atoms (that is located above that N_4-plane) in the second porphyrin unit.

[13] M. Zerner, M. Gouterman, *Theor. Chim. Acta* **1966**, *4*, 44–63.

[14] In effect this is a manifestation of the cation-π interaction (D. A. Dougherty, *Science* **1996**, *271*, 163), with the nearby π system appearing to act as a weak fifth ligand for the Zn atom. The Zn–π distance is much greater than in a conventional Zn–O bond so it is not surprising that we detect no displacement of the metal from the porphyrin plane.

[15] The possible π–π interaction between porphyrins p2 and p3 in complex **4** (Figure 5) is probably weak (if it exists at all), given the geometrical relationship, and therefore it is not expected to significantly change the Lewis acidity of the Zn atoms.

[16] Due to binding of a methanol molecule to a zinc porphyrin, the Zn atom lies at a mean distance of about 0.2 Å above the N_4 plane towards the oxygen atom. Therefore, as only one methanol molecule is bound to the zinc atom from within the cavity of **1**, while two molecules of methanol are bound, one inside and one outside, the cavity of **1a** and **1b**, the effective difference in the distance between the two centre points of the N_4 planes in the various receptors should correspondingly be corrected.

[17] This is similar to the known observation that *meso*-configurations can have enantiomeric conformers in crystals: for example, in the crystalline state xylitol has the bent-chain *enantiomorphic* conformation; it crystallises in the $P2_12_12_1$ space group, so each crystal contains either only optically active left-handed or the optically active right-handed conformers. There are, of course, an equal number of left- and right-handed crystals in any one batch, which on dissolution give no optical activity; see: G. A. Jeffrey and W. Saenger, *Hydrogen Bonding in Biological Structures*, Springer, Berlin, **1991**, p. 175.

[18] As the directional properties in hydrogen bonding of the O–H···O type are very soft (see: R. Taylor, O. Kennard, *Acc. Chem. Res.* **1984**, *17*, 320–326), this gives further confidence for hydrogen bonding in the framework drawn in Figure 6.

[19] As the precision in the location of hydrogen atoms is less than for oxygen atoms, we present the O···O distances. However, Figure 6 represents the observed relative orientation of the hydrogen bonding in complex **4**.

[20] a) K. K. Chacko, W. Saenger, *J. Am. Chem. Soc.* **1981**, *103*, 1708; b) G. A. Jeffrey, A. Robbins, *Acta Crystallogr. Sect. B* **1978**, *34*, 3817–3820.

[21] a) J. E. H. Koehler, B. Lesyng, W. Saenger, *J. Comput. Chem.* **1987**, *8*, 1090–1098; b) B. Lesyng, W. Saenger, *Biochim Biophys. Acta* **1981**, *678*, 408.

[22] C. B. Aakeröy, K. R. Seddon, *Chem. Soc. Rev.* **1993**, *22*, 397–407.

[23] R. P. Bonar-Law, J. K. M. Sanders, *J. Am. Chem. Soc.* **1995**, *117*, 259–271.

[24] G. R. Desiraju, *Angew. Chem.* **1995**, *107*, 2541–2558; *Angew. Chem. Int. Ed. Engl.* **1995**, *34*, 2311–2327.

[25] A. Nangia, G. R. Desiraju, *Chem. Commun.* **1999**, 605–606.

[26] As the N_4 planes in porphyrins p2 and p3 deviate by 2.3(5)° from being parallel, the distance between these planes was calculated as the average of the distances between each of the nitrogen atoms in porphyrins p2 and p3 and the N_4 plane in porphyrins p3 and p2, respectively.

[27] π–π interactions between coordinated pyridine ligands and between these ligands and a pyrrole unit of porphyrins, in a cyclic metalloporphyrin trimer, were believed to be the driving force for the formation of an interpenetrated dimer of trimers in the solid state: H. L. Anderson, A. Bashall, K. Henrick, M. McPartlin, J. K. M. Sanders, *Angew. Chem.* **1994**, *106*, 445–447; *Angew. Chem. Int. Ed. Engl.* **1994**, *33*, 429–431.

[28] M. M. Harding, *J. Synchrotron Rad.* **1996**, *3*, No.Pt6, 250–259.

[29] R. J. Cernik, W. Clegg, C. R. A. Catlow, G. Bushnell-Wye, J. V. Flaherty, G. N. Greaves, M. Hamichi, I. D. Borrows, D. J. Taylor, S. J. Teat, *J. Synchrotron Rad.* **1997**, *4*, 279–286.

[30] W. Clegg, M. R. J. Elsegood, S. J. Teat, C. Redshaw, V. C. Gibson, *J. Chem. Soc. Dalton Trans.* **1998**, 3037–3039.

[31] SMART (control) and SAINT (integration) software, version 4, Bruker AXS Inc., Madison, WI 1994.

[32] G. M. Sheldrick, SADABS, program for scaling and correction of area detector data, University of Göttingen, **1997** (based on the method of R. H. Blessing, *Acta Crystallogr.* Sect A **1995**, *51*, 33–38).

[33] W. Clegg, LSCELL, program for refinement of cell parameters from SMART data, University of Newcastle upon Tyne, **1995**.

[34] S. L. Darling, C. C. Mak, N. Bampos, N. Feeder, S. J. Teat, J. K. M. Sanders, *New J. Chem.* **1999**, *23*, 359–364.

[35] H.-J. Kim, J. E. Redman, M. Nakash, N. Feeder, S. J. Teat, J. K. M. Sanders, *Inorg. Chem.* **1999**, *38*, 5178–5183.

[36] A. Altomare, G. Cascarano, C. Giacavazzo, A. Guagliardi, M. C. Burla, G. Polidori M. C. Camalli, *J. Appl. Crystallogr.* **1994**, *27*, 435.

[37] G. M. Sheldrick, SHELXL93, Program for the Refinement of Crystal Structures, Universität Göttingen, Germany, **1997**.

Received: December 20, 1999 [F2197]